CARBON 62 (2013) 35–42

Available at www.sciencedirect.com
SciVerse ScienceDirect
journal homepage: www.elsevier.com/locate/carbon

Developing high-performance aluminum matrix composites with directionally aligned carbon nanotubes by combining friction stir processing and subsequent rolling

Z.Y. Liu, B.L. Xiao, W.G. Wang [1], Z.Y. Ma *

Shenyang National Laboratory for Materials Science, Institute of Metal Research, Chinese Academy of Sciences, 72 Wenhua Road, Shenyang 110016, China

A R T I C L E I N F O

Article history:
Received 25 March 2013
Accepted 26 May 2013
Available online 4 June 2013

A B S T R A C T

A route combining friction stir processing and subsequent rolling processing was established to fabricate 1.5–4.5 vol.% carbon nanotube (CNT)-reinforced 2009Al composites. Microstructural observations indicated that CNTs were individually dispersed and directionally aligned in the aluminum matrix of the CNT/2009Al composites. The tube structure of the CNTs was retained and the CNT–Al interface was bonded without pores. As a result, great increases in yield strength, ultimate tensile strength, and Young's modulus were achieved when a higher concentration of CNTs was incorporated. Moreover, the composites exhibited good ductility. In particular, 3 vol.% CNT/2009Al composite exhibited an ultimate tensile strength of 600 MPa and elongation of 10%, much higher strength–ductility than the corresponding values for CNT/Al composites fabricated by other processes.

1. Introduction

The incorporation of reinforcements into structural materials is a promising way to produce stronger materials with higher strength and stiffness [1–5]. As a new type of reinforcement, single- and multi-walled carbon nanotubes (CNTs) have created tremendous expectations as strengthening additives for metal matrix composites due to their extremely high strength (>30 GPa) and modulus (about 1 TPa) [6–12]. Investigations of CNT/metal composites have been increasing since the first article was published in 1998 [13]. However, no real improvement in the mechanical properties of CNT/metal composites was reported before 2005, essentially due to the challenges of (1) dispersing the CNTs in the metal matrix, (2) aligning the CNTs in the metal matrix, and (3) obtaining good bonding between the CNTs and metal.

In the past decade, several routes, such as roll-bonding, molecular-level mixing and ball milling, have been tried to fabricate CNT/metal composites. By using roll-bonding method, CNT/Al composites with CNT contents of 2–9.5 vol.% were fabricated [14]. Fifty nine percentage Young's modulus increase and 250% tensile strength increase were obtained for 2 vol.% CNT/Al and 4.5 vol.% CNT/Al, respectively. However, the CNT clusters with micro-meter size were observed for high CNT concentration composites.

By means of "molecular-level mixing", that is, chemical reactions between functionalized CNTs and metal (Cu, Co, Ni) ions, composites with uniformly dispersed CNTs were

* *Corresponding author*: Fax: +86 24 83978908.
E-mail address: zyma@imr.ac.cn (Z.Y. Ma).
[1] Now is with Liaoning Shihua University.
0008-6223/$ - see front matter
http://dx.doi.org/10.1016/j.carbon.2013.05.049

prepared [15]. However, transferring this method to CNT-reinforced aluminum or magnesium matrix composites was hardly compatible with industrial production routes.

By using ball milling, CNTs could be uniformly distributed in the metal matrix due to the process of repeated deformation, cold welding, and fracturing of the metal powders [16–20]. Although the ball-milling process is one of the most promising routes for preparing CNT/metal composites, it would contaminate the composite powders and cause severe damage to the CNTs because of its large energy input as well as the lengthy treatment time [21,22]. The duration of ball milling and energy input during ball milling for the fabrication of CNT/Al composites need to be strictly controlled.

Friction stir processing (FSP), a development based on the basic principles of friction stir welding, is a relatively new metal-working technique [23]. The basic concept of FSP is remarkably simple. A non-consumable rotating tool with a specially designed pin and shoulder is inserted into the workpiece and traverses a desired path to cover the region of interest. The tool heats the workpiece due to the friction between the tool and workpiece and the plastic deformation of the material and drives the softened material to flow around the pin. The combination of tool rotation and translation results in the movement of material from the front to the back of the pin. Thus, the material in the processed zone is severely deformed and thoroughly mixed in solid state, achieving localized microstructural modification which enhances specific properties.

FSP has been demonstrated to be an effective method of incorporating reinforcing particles, for example nano-sized particles, into the metal matrix, and homogenizing the microstructure of heterogeneous materials such as cast alloys and composites [24–26]. Izada et al. fabricated CNT/Al composites with CNT content as high as 50 vol.% using a FSP method [27]. The hardness increased by ~200% compared to that of the Al matrix due to uniformly dispersed CNTs. However, the tensile properties of the CNT/Al composites were not reported. Our previous investigation also indicated that CNTs could be uniformly dispersed into the aluminum matrix by a modified FSP route [28]. However, the CNTs were randomly arranged in the FSP composites, which limited the improvement in the strength and ductility of the fabricated composites.

Plastic deformation, such as hot extrusion or hot rolling, can achieve alignment of short fibers or whiskers in the metal matrix [29], and has therefore been used as a subsequent processing route for CNT/Al composite fabrication. Choi et al. [30] used hot rolling to carry out densification and CNT-alignment of ball-milled CNT/Al powders. The strength of the CNT/Al composite with aligned CNTs was greatly increased, but the elongation (2–6%) was not satisfactory, which was considered to be the result of contamination (by Al_2O_3, Fe, etc.) and the extremely refined grain size (~200 nm) induced by ball milling. For the CNT/Al composites fabricated by FSP, which led to much less contamination and relatively large grain sizes (0.8–2 μm), higher strength and good ductility are expected if the CNTs can be aligned.

In this work, fabrication processing of CNT/aluminum composites based on FSP and hot plastic deformation was used. Firstly, CNT-reinforced 2009Al composites were fabricated using a conventional powder metallurgy process to form bulk billets. Then, the billets were subjected to FSP to improve the distribution of the CNTs. Finally, the processed composites were subjected to hot rolling to align the CNTs. This work aims to establish an effective route for aligning the dispersed CNTs in the aluminum matrix and obtaining composites with excellent strength as well as ductility.

2. Experimental

2.1. *Raw materials and composite billet fabrication*

The as-received CNTs (95–98% purity) provided by Tsinghua University had entangled morphologies with an outer diameter of 10–20 nm and a length of several microns (Fig. 1). No extra pre-treatments of the CNTs were conducted. First, 1.5, 3, and 4.5 vol.% CNTs were mixed with 2009Al alloy (Al-4.5 wt.% Cu-1.2 wt.% Mg) powders, with an average diameter of 10 μm, in a bi-axis rotary mixer at 50 rpm for 8 h at a ball-to-powder ratio of 1:1. The as-mixed powders were cold-compacted in a cylinder die under a pressure of about 10 MPa, degassed under vacuum of $\sim 5 \times 10^{-3}$ Pa, and hot pressed under a pressure of about 50 MPa at 833 K for 1 h into cylindrical billets with a diameter of 55 mm and a height of 50 mm.

2.2. *CNT dispersion by FSP*

The billets were then hot forged by steel canning at 723 K into disc plates with a thickness of about 10 mm. Then the plates were subjected to overlapping FSP (shown in Fig. 2(a)) at a tool rotation rate of 1200 rpm and a travel speed of 100 mm/min using a tool with a concave shoulder 20 mm in diameter and a threaded cylindrical pin 6 mm in diameter and 4.2 mm in length. To achieve integrity of the processed zone, two adjacent FSP zones were overlapped by 50%. To completely disperse the CNTs into the aluminum matrix, the tool offset was placed again to the original location for the second overlapping FSP treatment.

2.3. *CNT alignment by hot rolling*

The cross section of the FSP plate was etched using 10% NaOH aqueous solution. Thus the FSP zone could be easily

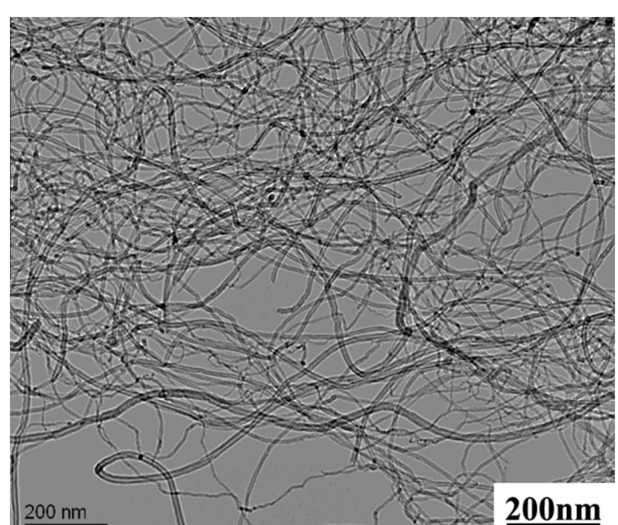

Fig. 1 – Morphology of the as-received CNTs.

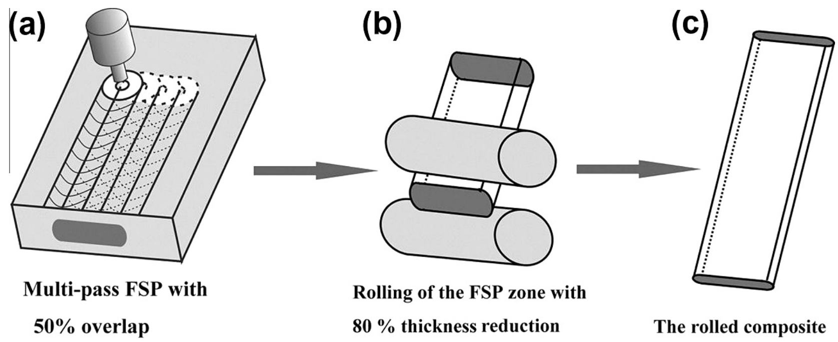

Fig. 2 – Schematic of the CNT/2009Al composite fabrication flow.

indentified and then the surrounding material was machined away. To align the CNTs in the aluminum matrix, the FSP zone was then hot rolled at 753 K (Fig. 2(b)). The rolling was performed along the FSP direction several times, reducing the thickness by less than 20% each time. After each rolling pass, the composites were annealed at 753 K for 10 min. The total reduction in thickness was about 80%. Hot-rolled composite sheets (1.2 mm in thickness, ~200 cm^2 in area) were obtained (Fig. 2(c)). The composites were solution treated at 768 K for 1 h, quenched in water, and then aged naturally for four days.

2.4. *Characterization of the composites*

The CNT distributions in the matrix under various fabrication conditions were examined using scanning electron microscopy (SEM, Quanta 600), field emission SEM (Leo Supra), and transmission electron microscopy (TEM, Tecnai G2 20). The CNT–Al interface and CNT structure were observed by high resolution TEM (HRTEM, Tecnai G2 20).

The Young's modulus of the composites was measured by the ultrasonic-resonance method using RFDA-HTVP1750-C (IMCE). The specimens, which had dimensions of $40 \times 4 \times 1$ mm, were machined with the length parallel to the rolling direction for the rolled composites and parallel to the FSP direction for the FSP composites.

Tensile specimens with a gauge length of 5 mm, a width of 1.5 mm, and a thickness of 1 mm were machined from the rolled composites parallel to the rolling direction. Tensile tests were conducted at a strain rate of $1 \times 10^{-3}\,s^{-1}$ at room temperature using an Instron 5848 microtester. At least three specimens were tested for each composite. For the purpose of comparison, the tensile tests on the 2009Al and the FSP composites were conducted under the same conditions, with the gauge length parallel to the FSP direction.

3. Results and discussion

Fig. 3 shows the SEM images of the rolled composites. It can be seen that no CNT clusters were observed under SEM in the composites with CNT concentrations of 1.5–4.5 vol.%. The white phase was Al_2Cu that did not dissolve during solid-solution treatment and the black dots were etching pits. Higher magnification image shown in Fig. 3(d) indicates that the CNTs (marked by black arrow) were uniformly dispersed in the aluminum alloy matrix.

Fig. 4 shows the grain structures of the FSP-rolled composites. Grain refinement could be observed as the CNT concentration increased. The grain size of the 1.5 vol.% CNT/2009Al composite was about 3 μm. As the CNT concentration increased to 3 and 4.5 vol.%, the grain size decreased to about 0.8 and 0.5 μm, respectively. The grain refinement was attributed to the effective pinning effect of uniformly dispersed CNTs. Thus, the fine grain size could be retained even after solution treatment at 768 K for 1 h.

Fig. 5 shows the CNT distribution in the FSP-rolled 4.5 vol.% CNT/2009Al composite. Two phenomena could be observed, the first being that most of the CNTs were uniformly dispersed in the 2009Al matrix, although a few nano-sized CNT entangles still could be observed at some places. This agreed with the SEM observation, shown in Fig. 3. Secondly, the CNTs were generally aligned along the rolling direction. This is attributed to the plastic deformation during hot rolling. In the FSP stage, the CNT clusters were broken down and the CNTs were cut shorter. The shorter CNTs were able to flow and rotate with the plastic deformation of the 2009Al alloy during hot rolling.

Fig. 6(a) shows a TEM image of the FSP-rolled 4.5 vol.% CNT/2009Al composite under a higher magnification. Singly dispersed CNTs with integrated tube morphology could be observed. The interface between the CNT wall and Al was clean and well bonded without defects. The interface between the reinforcement and the matrix played an important role in load transfer as the stress was transferred from the matrix to the reinforcement. A well-bonded CNT–Al interface without defects is beneficial for obtaining excellent tensile properties in the composites [31]. At the site of the CNT cap, no carbides were observed, although it has been reported that the carbon atoms at this location have stronger reaction activity [32]. However, Al_4C_3 phase was found at the tips of the CNTs (Fig. 6(a)). These tips were mainly formed due to shortening of the CNTs by strong shear strain at the FSP stage, and thus many defects formed at the CNT tips. The carbon atoms at the CNT tips reacted easily with aluminum to form Al_4C_3 in the subsequent processes or solution treatment.

The HRTEM image in Fig. 6(b) shows the CNT in the FSP-rolled 4.5 vol.% CNT/2009Al composite, further proving the good bonding of the CNT–Al interface. Also, the CNT had good structural integrity, with the tube structure being retained. This is of significant importance as the structural integrity has a great influence on the strength of the CNT itself and is beneficial for reducing the stress concentration; thus it

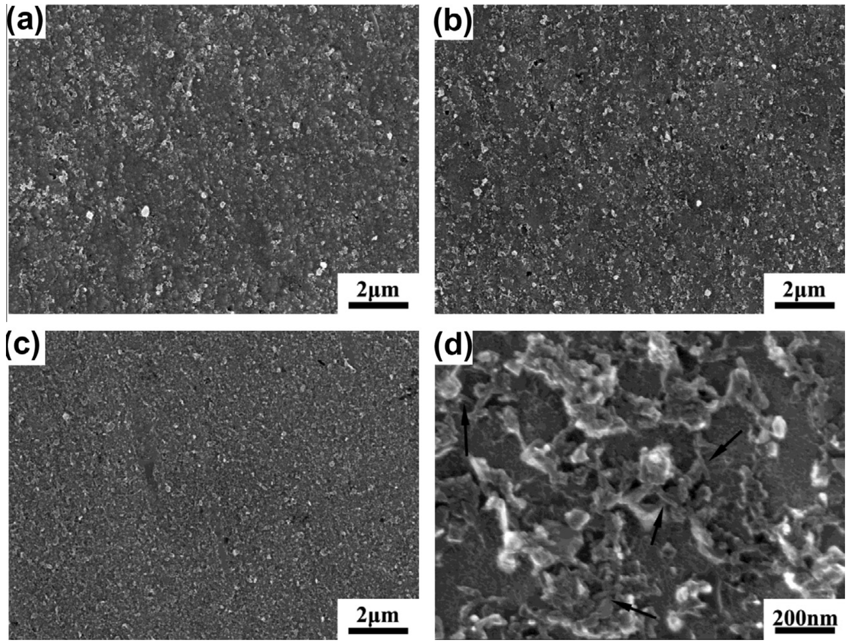

Fig. 3 – SEM images showing no CNT clusters in FSP-rolled CNT/2009Al composites with CNT concentrations of (a) 1.5, (b) 3, (c) and (d) 4.5 vol.%.

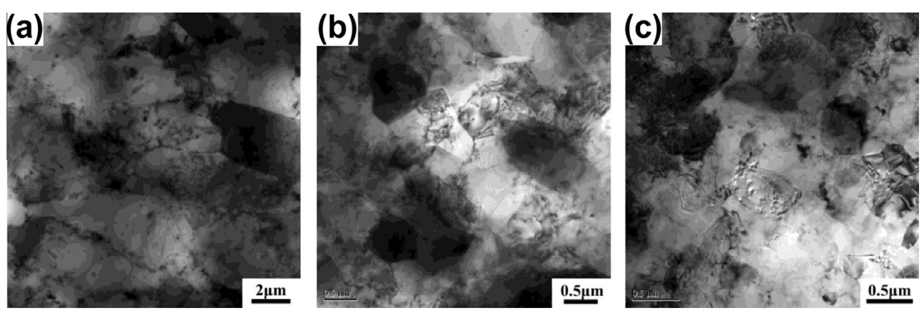

Fig. 4 – TEM images showing grains of FSP-rolled CNT/2009Al composites with CNT concentrations of (a) 1.5, (b) 3, and (c) 4.5 vol.%.

could improve the tensile properties of the CNT/metal composites.

Fig. 7 shows the stress–strain curves of the rolled CNT/2009Al composites. Both the yield strength (YS) and the ultimate tensile strength (UTS) of the composites were significantly enhanced by the incorporation of the CNTs and increased as the CNT content increased. The YS values of the 3 and 4.5 vol.% CNT/2009Al composites reached 470 and 570 MPa, and the UTS values were as high as 600 and 640 MPa. The elongation of the composites decreased because of the incorporation of CNTs. This is attributed to the fracture mode of the composites. The composite fracture is directly related to the cracking of the reinforcement and interfacial failure. In the composites with higher fractions of CNTs, voids tended to form at low strain during tension due to the transfer of stress at the reinforcement–matrix interfaces, resulting in a lower level of elongation compared with the alloy matrix. It is noted that the FSP-rolled composites could still exhibit excellent ductility. The 3 and 4.5 vol.% CNT/2009Al composites exhibited elongation of 10% and 5%.

It is noted that the stress–strain curves of the composites exhibited work hardening factors similar to that of the alloy matrix. This implies that the fine grain size of 0.5–3 μm could still retain the relatively high storage capability of dislocations and the aligned CNTs did not result in a more severe dislocation multiplication compared with the 2009Al matrix. However, dislocation density increase induced by CNTs and corresponding strain hardening were observed in rolled CNT reinforced aluminum matrix composites [14]. This difference should be attributed to that the FSP-rolled composites were solution treated at 768 K for 1 h, resulting in annihilation of the multiplicated dislocations at the high temperature. A tip drop phenomenon was also found in the stress–strain curves of the FSP-rolled composites in Fig. 7, especially the composite with 4.5 vol.% CNT. This will be discussed later.

Fig. 8 shows the tensile properties of the CNT/2009Al composites fabricated by FSP and FSP-rolling processes. The strength values of the FSP-rolled composites were much higher than those of the FSP composites, especially the UTS. For the FSP composites, the UTS decreased as the CNT concentra-

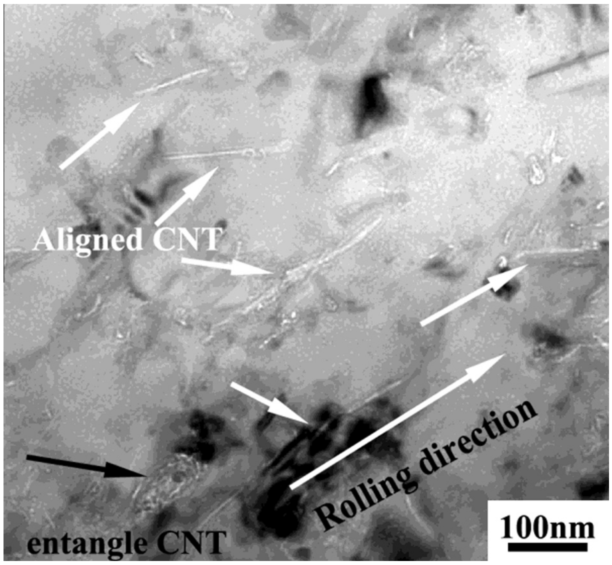

Fig. 5 – TEM image showing CNT distribution and CNT alignment in FSP-rolled 4.5 vol.% CNT/2009Al composite.

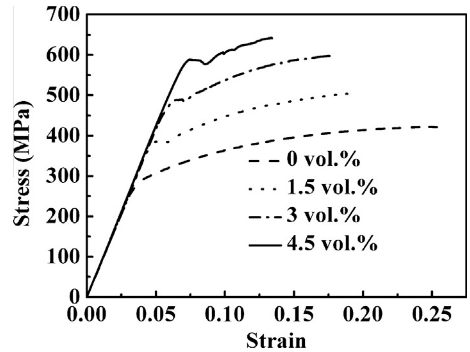

Fig. 7 – Stress–strain curves of FSP-rolled CNT/2009Al composites with different CNT concentrations.

tion increased from 1.5 to 4.5 vol.%. However, the UTS of the FSP-rolled composites increased further as the CNT concentration increased to 4.5 vol.%. The elongation and modulus of the FSP-rolled composites were much higher than those of the FSP composites with the same CNT concentrations, which were considered to be the result of the CNT alignment. It should be mentioned that the plotted Young's modulus values were determined by vibration testing and the stress–strain curves in Fig. 7 were obtained without using extensometer, thus the slopes of various stress–strain curves did not exhibit obvious difference.

FSP-rolled composites, and (c) elastic modulus comparison between FSP and FSP-rolled composites.

In our previous investigation of FSP CNT/2009Al composites [28], a strengthening model was proposed to predict the YS of the CNT/Al composites with individually dispersed CNTs based on load transfer theory and the Hall–Petch relationship:

$$\sigma_c = (\sigma_0 + kd^{-1/2})[V_f(s+4)/4 + (1 - V_f)] \quad (1)$$

where σ_c is the YS of the composite, σ_0 is rationalized as either a frictional stress in response to the motion of dislocation glide or an internal back stress, d is the matrix grain size in the composite, k is the Hall–Petch slope (for Al–Cu–Mg alloy it is about 0.1 MPa $m^{1/2}$ [28]), s is the effective aspect ratio of the CNTs, and V_f is the volume fraction of CNTs.

Table 1 shows a comparison between the YS values obtained experimentally and those calculated using Eq. (1). It is noted that the calculated results are in good agreement with the experimental ones. Thus, it can be concluded that the CNT/2009Al composites were mainly strengthened by both the load transfer from the matrix to the CNTs and the grain refinement of the alloy matrix. According to Eq. (1), the aspect ratio s of the CNTs has a great influence on the strength of the composites. A larger aspect ratio led to higher strength of the composites. For the FSP composites with randomly distributed CNTs, the effective aspect ratio was only one half of the actual aspect ratio of the CNTs [28,29]. However, for the FSP-rolled composites with directionally aligned CNTs, the effective aspect ratio was almost equal to the actual aspect ratio of the CNTs. Thus, according to Eq. (1), a much higher load transfer efficiency of the CNTs could be obtained in the FSP-rolled composites. Thus, the FSP-rolled composites achieved much higher strengths compared with the FSP composites.

The strength and elongation of CNT-reinforced pure Al and Al–4 wt.% Cu composites fabricated by various methods are compared in Fig. 9. It can be seen that CNT-reinforced Al or

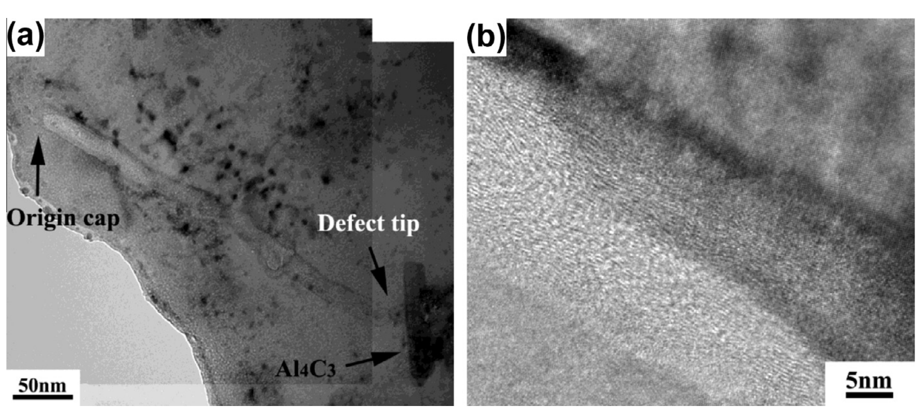

Fig. 6 – (a) TEM image showing CNT–Al interface with good bonding and (b) HRTEM image showing CNT tube structure.

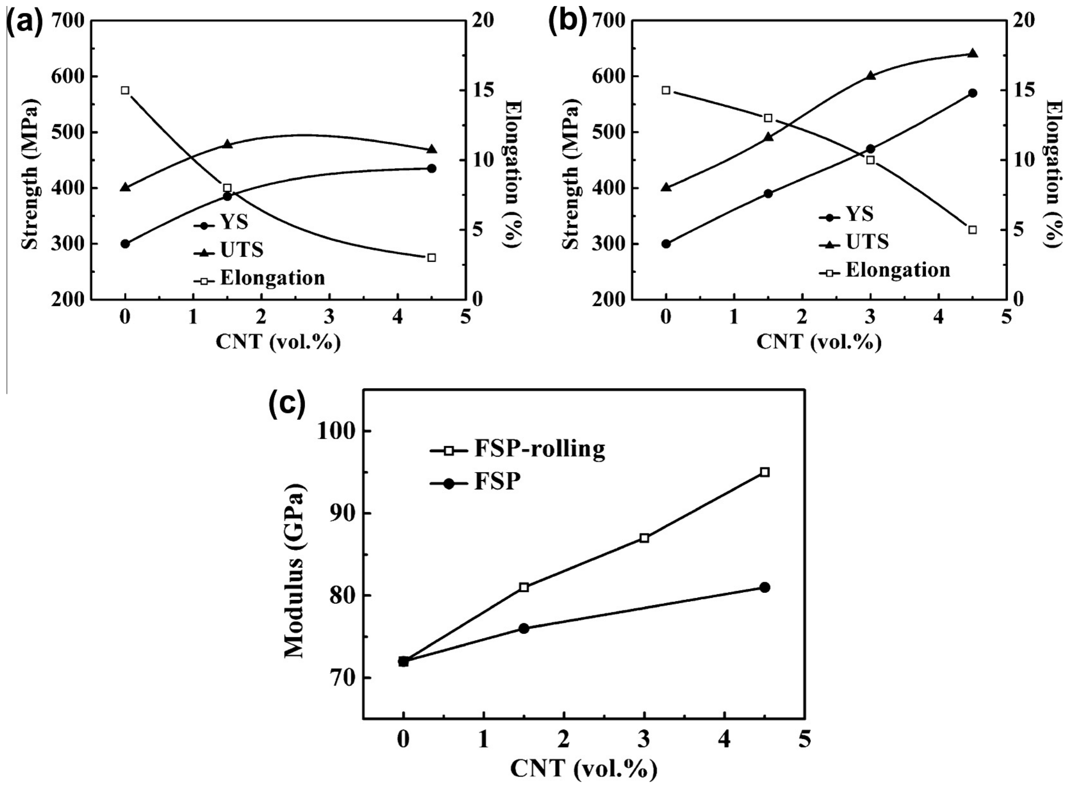

Fig. 8 – Tensile properties of CNT/2009 Al composites: (a) FSP composites, (b) FSP-rolled composites, and (c) elastic modulus comparison between FSP and FSP-rolled composites.

Table 1 – Experimental and calculated YS of FSP-rolled CNT/2009Al composites.

CNT (vol.%)	*d* (nm)	s	Experimental YS (MPa)	Calculated YS (MPa)
0	4000	–	310	–
1.5	3000	30	380	359
3	800	30	470	464
4.5	500	30	570	552

Al alloy composites had a strength–ductility trade-off; that is, high strength was accompanied by low ductility, no matter what fabrication route and matrix were used. However, the FSP-rolled CNT/2009Al composites exhibited both high strength and good ductility, indicating the possibility of retaining good ductility in CNT/Al alloy composites. This can be attributed to the following three factors.

Firstly, the CNTs were uniformly dispersed and generally aligned along the rolling direction. This avoids the preferential fracture problems induced by CNT clusters and the non-simultaneous CNT debonding associated with randomly oriented CNTs. Secondly, the grain sizes of the composites ranged from sub-micro (~500 nm) to several micrometers (~3 μm). The relatively large grains were able to retain good strain-hardening capacity and could therefore retain a large number of dislocations inside the grains during tension. This judgment is supported by similar work-hardening factors in the stress–strain curves of the FSP-rolled CNT/2009Al composites and the 2009Al alloy. Thirdly, no contamination, for example by Al_2O_3 or Fe, was introduced into the present composites during processing. Contamination is usually a significant problem in ball-mill processing and flaky powder metallurgy processing.

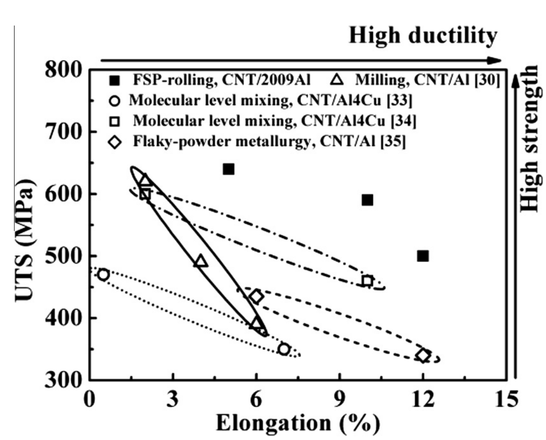

Fig. 9 – Strength–ductility comparison of CNT/Al composites fabricated by various methods. The data were plotted based on [30,33–35].

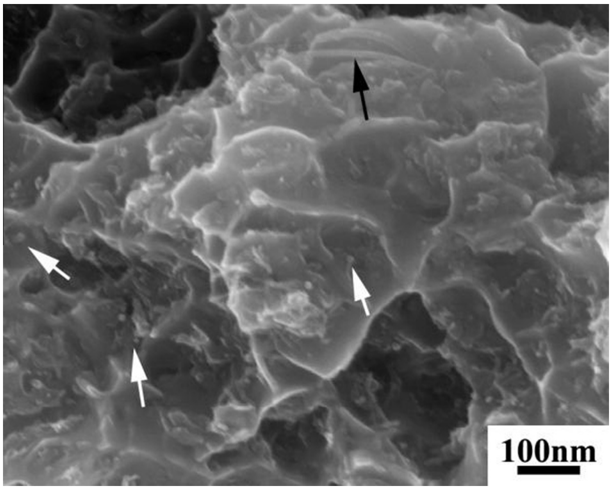

Fig. 10 – Tensile fractograph of FSP-rolled 4.5 vol.% CNT/2009Al composite.

Fig. 10 shows a tensile fractograph of the FSP-rolled 4.5 vol.% CNT/2009Al composite. The pulled-out CNTs were observed to be uniformly dispersed on the fracture surface, indicating that the clustering problem was successfully solved by using the FSP and subsequent rolling processes. The pulled-out CNTs on the fracture surfaces could be divided into two types. One was CNTs with only their tips emerging from the fracture surfaces, as marked by white arrows in Fig. 10. The other was CNTs with long pulled-out lengths of about 200 nm, marked by the black arrow in Fig. 10.

For short fiber-reinforced composites, an applied force can be transferred from the matrix to the short fibers by shear stresses that are developed along the fiber–matrix interfaces. In this case, it generates variation in the stress along the length of the fiber, and the stress of the short fibers increases proportionally from the fiber end to reach a maximum value at the mid-length. Thus, the CNT–Al interfaces at the site of the mid-length failed easily and then cracks developed along the interfaces. The long pulled-out CNTs formed subsequently on the fracture surfaces. On the other hand, the interface on the CNT tip was another site at which preferential crack occurred easily. As these places had higher stress triaxiality due to the formation of Al_4C_3 and stress states, they could lead to the formation of micro-pores. As the stress at the CNT tip increased to a critical value, micro-pores formed at this place. Thus, a tip drop formed on the stress–strain curve. This type of micro-pore at the CNT tip was of nanometer size. That is, the damaged region was smaller and was possibly even below the critical flaw size at which cracking can start. As a result, the CNTs with damaged tip interfaces could still transfer load and further strengthen the Al matrix.

4. Conclusions

FSP plus subsequent hot rolling was successfully used to fabricate 1.5–4.5 vol.% CNT/2009Al composites with uniformly dispersed and directionally aligned CNTs. The CNT–Al interfaces were well bonded and the tube structure of the CNT was retained, although some Al_4C_3 formed at the CNT tips.

The YS and UTS values of the FSP-rolled CNT/2009Al composites were significantly higher than those of the matrix alloy. Compared with the FSP composites with randomly distributed CNTs, the FSP-rolled composites with directionally aligned CNTs exhibited much higher strength, ductility, and modulus values.

The CNT/2009Al composites fabricated by the FSP-rolling processes exhibited excellent strength–ductility compared with the CNT/Al composites fabricated by other processes. In particular, the FSP-rolled 3 vol.% CNT/2009Al composite exhibited a UTS of 600 MPa along with a higher elongation of 10%.

Acknowledgments

The authors gratefully acknowledge the support of (a) the National Basic Research Program of China under Grant nos. 2011CB932603 and 2012CB619600 and (b) the National Natural Science Foundation of China under Grant no. 50890171.

REFERENCES

[1] Torralba JM, da Costa CE, Velasco F. P/M aluminum matrix composites: an overview. J Mater Process Technol 2003;133(1–2):203–6.
[2] Miracle DB. Metal matrix composites – from science to technological significance. Compos Sci Technol 2005;65(15–16):2526–40.
[3] Moya JS, Lopez-Esteban S, Pecharroman C. The challenge of ceramic/metal microcomposites and nanocomposites. Prog Mater Sci 2007;52(7):1017–90.
[4] Rosso M. Ceramic and metal matrix composites: routes and properties. J Mater Process Technol 2006;175(1–3):364–75.
[5] Shorowordi KM, Laoui T, Haseeb ASMA, Celis JP, Froyen L. Microstructure and interface characteristics of B_4C, SiC and Al_2O_3 reinforced Al matrix composites: a comparative study. J Mater Process Technol 2003;142(3):738–43.
[6] Trojanowicz M. Analytical applications of carbon nanotubes: a review. TrAC, Trends Anal Chem 2006;25(5):480–9.
[7] Terrones M. Scinece and technology of the 21st century: synthesis, properties, and applications of carbon nanotubes. Annu Rev Mater Res 2003;33(1):419–501.
[8] Bakshi SR, Lahiri D, Agarwal A. Carbon nanotube reinforced metal matrix composites – a review. Int Mater Rev 2010;55:41–64.
[9] Curtin WA, Sheldon BW. CNT-reinforced ceramics and metals. Mater Today 2004;7(11):44–9.
[10] Thostenson ET, Ren Z, Chou T-W. Advances in the science and technology of carbon nanotubes and their composites: a review. Compos Sci Technol 2001;61(13):1899–912.
[11] Ajayan P, Zhou O. Applications of carbon nanotubes. Top Appl Phys 2001;80:391–425.
[12] Demczyk BG, Wang YM, Cumings J, Hetman M, Han W, Zettl A, et al. Direct mechanical measurement of the tensile strength and elastic modulus of multiwalled carbon nanotubes. Mater Sci Eng A 2002;334(1–2):173–8.
[13] Kuzumaki T, Miyazawa K, Ichinose H, Ito K. Processing of carbon nanotube reinforced aluminum composite. J Mater Res 1998;13(9):2445–9.
[14] Lahiri D, Bakshi SR, Keshri AK, Liu Y, Agarwal A. Dual strengthening mechanisms induced by carbon nanotubes in

roll bonded aluminum composites. Mater Sci Eng A 2009;523(1–2):263–70.
[15] Jeong YJ, Cha SI, Kim KT, Lee KH, Mo CB, Hong SH. Synergistic strengthening effect of ultrafine-grained metals reinforced with carbon nanotubes. Small 2007;3(5):840–4.
[16] Esawi AMK, El Borady MA. Carbon nanotube-reinforced aluminum strips. Compos Sci Technol 2008;68(2):486–92.
[17] Esawi AMK, Morsi K, Sayed A, Taher M, Lanka S. Effect of carbon nanotube (CNT) content on the mechanical properties of CNT-reinforced aluminum composites. Compos Sci Technol 2010;70(16):2237–41.
[18] Wang L, Choi H, Myoung J-M, Lee W. Mechanical alloying of multi-walled carbon nanotubes and aluminum powders for the preparation of carbon/metal composites. Carbon 2009;47(15):3427–33.
[19] Stein J, Lenczowski B, Fréty N, Anglaret E. Mechanical reinforcement of a high-performance aluminum alloy AA5083 with homogeneously dispersed multi-walled carbon nanotubes. Carbon 2012;50(6):2264–72.
[20] Morsi K, Esawi AMK, Lanka S, Sayed A, Taher M. Spark plasma extrusion (SPE) of ball-milled aluminum and carbon nanotube reinforced aluminum composite powders. Composites Part A 2010;41(2):322–6.
[21] Kónya Z, Zhu J, Niesz K, Mehn D, Kiricsi I. End morphology of ball milled carbon nanotubes. Carbon 2004;42(10):2001–8.
[22] Pierard N, Fonseca A, Konya Z, Willems I, Van Tendeloo G, Nagy JB. Production of short carbon nanotubes with open tips by ball milling. Chem Phys Lett 2001;335(1–2):1–8.
[23] Mishra RS, Ma ZY. Friction stir welding and processing. Mater Sci Eng R 2005;50(1–2):1–78.
[24] Ma ZY, Pilchak AL, Juhas MC, Williams JC. Microstructural refinement and property enhancement of cast light alloys via friction stir processing. Scr Mater 2008;58(5):361–6.
[25] Morisada Y, Fujii H, Nagaoka T, Fukusumi M. Nanocrystallized magnesium alloy – uniform dispersion of C60 molecules. Scr Mater 2006;55(11):1067–70.
[26] Mishra RS, Ma ZY, Charit I. Friction stir processing: a novel technique for fabrication of surface composite. Mater Sci Eng A 2003;341(1–2):307–10.
[27] Izadi H, Gerlich AP. Distribution and stability of carbon nanotubes during multi-pass friction stir processing of carbon nanotube/aluminum composites. Carbon 2012;50(12):4744–9.
[28] Liu ZY, Xiao BL, Wang WG, Ma ZY. Singly dispersed carbon nanotube/aluminum composites fabricated by powder metallurgy combined with friction stir processing. Carbon 2012;50(5):1843–52.
[29] Hong SH, Chung KH, Lee CH. Effects of hot extrusion parameters on the tensile properties and microstructures of SiCw-2124Al composites. Mater Sci Eng A 1996;206(2):225–32.
[30] Choi HJ, Shin JH, Min BH, Park JS, Bae DH. Reinforcing effects of carbon nanotubes in structural aluminum matrix nanocomposites. J Mater Res 2009;24(28):2610–6.
[31] Bakshi SR, Agarwal A. An analysis of the factors affecting strengthening in carbon nanotube reinforced aluminum composites. Carbon 2011;49(2):533–44.
[32] Ci L, Ryu Z, Jin-Phillipp NY, Rühle M. Investigation of the interfacial reaction between multi-walled carbon nanotubes and aluminum. Acta Mater 2006;54(20):5367–75.
[33] Nam DH, Cha SI, Lim BK, Park HM, Han DS, Hong SH. Synergistic strengthening by load transfer mechanism and grain refinement of CNT/Al–Cu composites. Carbon 2012;50(7):2417–23.
[34] Nam DH, Kim YK, Cha SI, Hong SH. Effect of CNTs on precipitation hardening behavior of CNT/Al–Cu composites. Carbon 2012;50(13):4809–14.
[35] Jiang L, Li Z, Fan G, Cao L, Zhang D. The use of flake powder metallurgy to produce carbon nanotube (CNT)/aluminum composites with a homogenous CNT distribution. Carbon 2012;50(5):1993–8.